

Complete and incomplete fusion cross sections for ${}^6\text{Li}+{}^{209}\text{Bi}$ reaction in multi-body classical molecular dynamical model

M. R. Morker, S. S. Godre*

Department of Physics, Veer Narmad South Gujarat University, Surat – 395007, India

* email: ssgodre@yahoo.com

Introduction

Heavy-ion reactions with weakly bound nuclei may result either in CF, or ICF processes involving fusion of only one of the projectile fragments. In a recent experiment [1] it is observed that direct processes such as nucleon transfer leading to breakup of the remaining projectile contribute significantly to the ICF processes. The usual calculations such as CDCC, semi-classical couple channel [2] or the Classical trajectory model [3] do not account for breakup following direct reactions in the ICF processes.

Using the multi-body Classical Molecular Dynamics simulation of ${}^6\text{Li}+{}^{209}\text{Bi}$ reaction it is shown that: (i) the breakup of a projectile fragment near the barrier leads to substantial increase in the ICF probabilities [4]; (ii) the expected increase in σ_{CF} on relaxation of the rigid-body (RB) constraint on the projectile is compensated by reduction in the flux leading to CF, due to ICF events [5]; (iii) the breakup probability increases with E_{CM} and, for given E_{CM} it also increases as b increases and peaks around some $b>0$ [6], while cross sections σ_{CF} and σ_{TF} were calculated for $b=0$ only [7]

Therefore, we present the results of σ_{CF} (Complete Fusion) and σ_{TF} (Total Fusion) calculations which are obtained at critical impact parameter, b_{cr} , where many ICF channels open up and compare with the calculations performed at $b=0$, where only few ICF channels open up.

Calculation Details

The weakly-bound ${}^6\text{Li}$ is constructed making use of the stable d and α with the energy between the fragments equal to -1.467 MeV.

The dynamical collision is carried out in the 3S-CMD model in 3-stages [5]: (1) Rutherford trajectory calculation up to $R_{\text{CM}}=2500$ fm for given E_{CM} and b ; (2) thereafter, assuming the

two nuclei as RB, using CRBD model calculation; (3) the RB constraints at about $R_{\text{CM}}=13$ fm are relaxed and the trajectories of all the nucleons are computed as in CMD model calculation. If one or both the projectile fragments are further constrained to be RB, then it is dynamically evolved as in the CRBD-model calculation.

We define CF (DCF+SCF) as an event in which all the projectile fragments are captured by the target for long intervals of time. ICF(x) is defined as an event where x is one of the fragments, or d , which is captured or x may also be $+n$, $+p$, n or p , when d also breaks up.

Barrier parameters for $b=0$ or b_{cr} for given E_{CM} and for a given initial orientation of the two nuclei are obtained for CF or ICF events from the dynamically generated ion-ion potential between the target and the projectile-fragments that are captured. The barrier parameters corresponding to $b=b_{\text{cr,CF}}$ or $b_{\text{cr,TF}}$ are used in the Wong formula [8] to calculate σ_{CF} or σ_{TF} .

Orientation-averaged fusion cross section is calculated from about 500-2000 Monte-Carlo sampled initial orientations for every E_{CM} . ICF cross section are calculated from $\sigma_{\text{TF}} = \sigma_{\text{CF}} + \sigma_{\text{ICF}}$. ICF events occurs at $b_{\text{cr,CF}} < b < b_{\text{cr,TF}}$.

Results and Discussion

In the present calculations, the bond between the two projectile fragments (d and α), as well as the target ${}^{209}\text{Bi}$, are kept non-rigid in the stage-3 for $R_{\text{CM}} < 13$ fm; while keeping α in the projectile fragment rigid.

σ_{CF} and σ_{TF} calculations for $b=0$ were reported in [7] and σ_{CF} with $b=b_{\text{cr,CF}}$ in [5]. We now calculate TF cross sections for $b=b_{\text{cr,TF}}$ and compare the results for CF and TF for central and non-central collisions.

Calculated σ_{CF} and σ_{TF} at $b=0$ for ${}^6\text{Li}+{}^{209}\text{Bi}$ reaction are shown in Fig. 1 and compared with the experimental CF and TF cross sections [9].

Experimental TF cross sections are obtained as a sum of the CF and ICF cross sections of ref [9]. The calculated cross sections with $b=0$ seem to match well with the experimental cross sections corresponding to CF and TF respectively, except at very low energies.

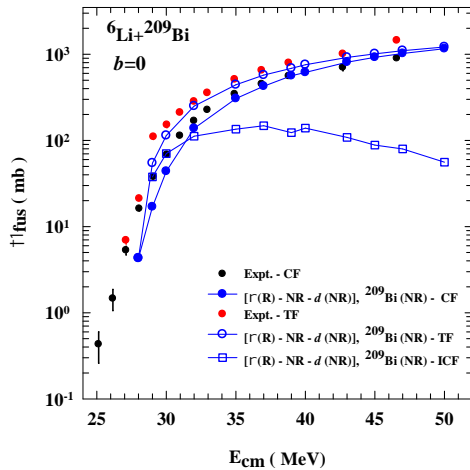


Fig. 1 CF, ICF and TF cross sections at $b=0$ [7]. (R- rigid body and NR -non rigid-body constrained).

Conventionally one uses the Wong’s formula [8] for fusion cross section calculations with $b=0$ approximation; which is justified at low energies. However, since at higher energies, higher partial wave contribution can not be neglected, we still use the Wong formula but with the barrier parameters corresponding to the higher partial wave or the critical impact parameter [10, 11]. Moreover, in the case of fusion reactions involving weakly bound projectiles, as shown in [6] the contribution of incomplete fusion increases at higher values of impact parameters, reaching a maximum and again diminishing at grazing impact parameters. Therefore, to obtain the effect of ICF events, the cross sections must include the contributions from trajectories with higher impact parameters.

The CF and TF cross sections calculated using the Wong formula with barrier parameters corresponding to the critical impact parameters b_{cr} for the particular events are shown in Fig. 2 and compared with the corresponding experimental data.

The difference in the TF and CF cross section corresponds to ICF cross sections which are

also shown in Fig. 1 and 2. The calculated ICF cross section in Fig. 2 corresponding to $b=b_{cr}$ is much larger at higher energies compared to the calculated ICF cross sections in Fig. 1 for $b=0$ case. This large difference arises because of the increased number of ICF events at $b>0$.

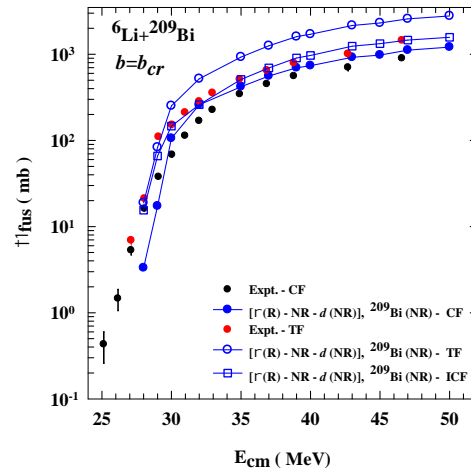


Fig. 2 CF [5], ICF and TF cross sections at b_{cr} . (R- rigid body and NR -non rigid-body constrained).

The CF and ICF cross sections in Fig. 2 are of the same order of magnitude, although CF cross sections in Fig. 2 are enhanced compared to those in Fig.1. The TF cross sections (Fig. 2) are also enhanced due to the enhanced values of ICF cross sections and are overestimated compared to the experimental values.

References

- [1] D H Luong *et al*, Phys Rev C **88**, 034609 (2013)
- [2] H D Marta *et al*, Phys Rev C **89**, 034625 (2014)
- [3] A Diaz-Torres *et al*, Phys Rev Lett **98**, 152701 (2007)
- [4] M R Morker, S S Godre, *this Proc.* (2015)
- [5] M R Morker, S S Godre, EPJ Web of Conf **86**, 28 (2015)
- [6] M R Morker, S S Godre, *Proc Symp on Nucl Phys* **59**,510 (2014)
- [7] M R Morker, S S Godre, *Proc Symp on Nucl Phys* **59**,524 (2014)
- [8] C Y Wong, Phys Rev Lett **31**, 766 (1973)
- [9] M Dasgupta *et al*, Phys Rev C **70**, 024606 (2004).
- [10] P R Desai, S S Godre, *Proc Symp on Nucl Phys* **55**,400 (2010)
- [11] N Rowley and K Hagino, Phys Rev C **91**, 044617 (2015)